RESEARCH ARTICLE

Experimental Design for Optimization of Felbamate Nanosuspension Using Box-Behnken Design

Poonam Maurya[1,2], Rishikesh Gupta[1*], Peeyush Bhardwaj[1], Purnima Tripathi[3], Alok Mahor[1], Raj Keshwar Prasad[2]

[1]*Institute of Pharmacy, Bundelkhand University, Jhansi, Uttar Pradesh, India.*
[2]*Shambhunath Institute of Pharmacy, Prayagraj, Uttar Pradesh, India.*
[3]*Anangpuria School of Pharmaceutical Sciences, Faridabad, Haryana, India.*

Received: 25th March, 2024; Revised: 10th July, 2024; Accepted: 15th August, 2024; Available Online: 31st August, 2024

ABSTRACT

Felbamate, a valuable antiepileptic drug, suffers from low water solubility and potential side effects, limiting its therapeutic application. This study addresses this challenge by developing a felbamate nanosuspension for nose-to-brain delivery using a three-factor, three-level Box-Behnken design. The research focused on identifying the optimal combination of key formulation variables, chitosan concentration, chitosan/sodium tripolyphosphate ratio, and Tween 80 surfactant concentration to achieve a nanosuspension with desirable particle size, polydispersity index, and high entrapment efficiency (%EE), all critical parameters for efficient drug delivery via the nasal route. The study identified an optimized formulation consisting of 0.176% chitosan, a 3.3:1 chitosan/TPP ratio, and 1.55% Tween 80 through rigorous experimentation and response surface methodology analysis. The optimized formulation yielded a nanosuspension of 115.0 ± 4.37 nm mean particle size, 0.118 ± 0.021 polydispersity index, and +34.08 ± 2.4 mV zeta potential, indicating a stable system with a narrow size distribution suitable for enhanced drug delivery. The entrapment efficiency of 93.18 ± 1.69% confirmed effective encapsulation, while *in-vitro* dissolution studies demonstrated a significantly higher dissolution rate compared to pure felbamate, suggesting improved bioavailability. The results emphasize the capacity of this optimized nanosuspension to improve the therapeutic efficacy of felbamate and hence justify additional preclinical and clinical research.

Keywords: Felbamate, Chitosan nanosuspension, Response surface methodology, Box-Behnken design, optimization.

International Journal of Pharmaceutical Quality Assurance (2024); DOI: 10.25258/ijpqa.15.3.41

How to cite this article: Maurya P, Gupta R, Bhardwaj P, Tripathi P, Mahor A, Prasad RK. Experimental Design for Optimization of Felbamate Nanosuspension Using Box-Behnken Design. International Journal of Pharmaceutical Quality Assurance. 2024;15(3):1349-1357.

Source of support: Nil.

Conflict of interest: None

INTRODUCTION

Felbamate, an antiepileptic drug known for its efficacy in treating refractory seizures, grapples with a significant limitation - its challenging solubility profile and first-pass metabolism.[1-3] The oral use of felbamate leads to inadequate absorption, resulting in uneven treatment outcomes and requiring higher doses to achieve the desired effect, therefore increasing the risk of undesirable side effects. Developing innovative formulations is crucial to reduce the negative effects of drugs and explore more targeted delivery methods.

This study focuses on a novel formulation, a felbamate nanosuspension designed for nose-to-brain drug delivery. Nanosuspensions address the limitations of felbamate by significantly enhancing the drug's solubility and dissolution rate. They increase the surface area of the drug particles, facilitating better absorption through the nasal mucosa and potentially improved bioavailability.[4,5] This improved formulation can lead to more consistent and reliable therapeutic effects, potentially lower dosing requirements, and a reduction in side effects, thereby enhancing patient compliance and overall treatment efficacy.[6] Additionally, the stability of the nanosuspension formulation ensures prolonged shelf life and effectiveness, making it a promising approach for optimizing Felbamate therapy.[7,8]

This study employed Response Surface Methodology (RSM) due to its well-established capability to optimize multiple variables and their interactions to achieve the desired formulation characteristics.[9,10] The methodology employs several experimental designs, formulates polynomial equations, and maps the response throughout the experimental domain to identify the optimal formulation(s), all rooted in the concept of design of experiments (DoEs).[11-13] RSM is used to

**Author for Correspondence: rishikeshgupt@gmail.com*

generate and optimize a felbamate chitosan nanosuspension, which may be more successful than conventional formulation due to its nose-to-brain targeting and fewer systemic side effects. Nanosuspension requires less expensive and sophisticated equipment than other drug delivery techniques. Optimization can reduce the number of experimental trials needed to formulate nanosuspension with optimal mean particle size, minimum polydispersity index (PDI), and maximum drug entrapment efficiency. This study aimed to formulate and optimize felbamate nanosuspension using a response surface approach using Box-Behnken Design. The optimized felbamate nanosuspension (FNS) formulation was tested for surface morphology, particle size, polydispersity index, drug entrapment, and *in-vitro* drug release.

MATERIALS AND METHODS

Materials

A free sample of felbamate was provided by Merck Ltd., Mumbai, India. Chitosan came from Wanbury Ltd. Mumbai, India. UK-based Aldrich Chemicals supplied sodium tripolyphosphate. S D Fine Chem. Ltd., Mumbai, India, supplied acetic acid and mannitol. All chemicals were of analytical quality and were used without any modifications. Design Expert 12.0.3.0 (Stat-Ease Inc., MN) was used to optimize the formulation.

Methods

Development of felbamate-loaded chitosan nanosuspension

Chitosan nanosuspension was prepared by ionic cross-linking of positively charged chitosan (CS) with tripolyphosphate (TPP) anions (Ionic gelation method).[5,14,15] In this method, CS solution was made in 1.5% v/v acetic acid and separately sodium TPP was made in distilled water. The addition of the surfactant Tween 80 was made to the CS solution. Subsequently, the sodium TPP solution was gradually introduced into the CS solution while slowly swirling with gentle magnetic stirring and sonication at ambient temperature. The cross-linking of CS by TPP produced the resulting CS nanosuspension. To form felbamate-loaded CS nanosuspension (FNS), the felbamate solution in polyethylene glycol-400 was added to the chitosan solution before the surfactant and TPP. The resulting FNS were concentrated using ultracentrifugation for 15,000 rpm at 4°C for 30 minutes. The liquid portion above the sediment was discarded, and the remaining material was used to determine the entrapment efficiency. The nanosuspension was freeze-dried using a lyophilizer to create freeze-dried nanoparticles (NPs) and kept for subsequent characterization experiments.[16]

The process variables (independent variables) that affected FNS particle size, PDI, and %EE were examined. To determine how different process variables affected the development of FNS, several experimental batches were produced using the formulas provided by Design Expert®. Characterization of the optimized FNS formulation assessed particle size, polydispersity index, drug entrapment efficiency, and drug release.

Experimental design using BBD

Statistical models were employed to optimize the felbamate nanosuspension. This study employed a 3-factor, 3-level BBD to develop polynomial models for the statistical optimization of formulation variables in the production of FNS. We utilized Design Expert® (Software Version 12.0.3.0, Stat-Ease Inc., MN) for this specific objective. The design consisted of five replicated central points and a cluster of points positioned at the midpoint of each side of the multidimensional cube. Empirical experiments were conducted to identify the distinct values of the independent variables. The chosen independent and dependent variables, together with their corresponding low (-1), medium (0), and high (+1) levels, are presented in Table 1. The selected independent variables for formulation were the concentration of the surfactant (CS) (X_1), the ratio of CS to TPP (X_2), and the concentration of the surfactant (Tween 80) (X_3). The dependent variables selected were the particle size (Y_1), the polydispersity index (Y_2), and the drug entrapment efficiency (EE%) (Y_3). The goal was to attain a high level of entrapment efficiency, a low polydispersity index (PDI), and an optimum particle size. The 17 formulas of the BBD-response surface methodology are listed in Table 2. An appropriate statistical model was defined as one with a p-value below 0.05. The R^2 statistical measure and analysis of variance (ANOVA) were used to validate the most suitable model. The results of these trials were analyzed using ANOVA, a statistical method that determined the importance of components and the interactions between them.

The polynomial model was used to represent the responses (Y_1, Y_2, and Y_3). This model was produced using the response surface approach and Design Expert® software. The model is provided below:

$$Y= b_0 + b_1X_1 + b_2X_2 + b_3X_3 + b_{12}X_1X_2 + b_{13}X_1X_3 + b_{23}X_2X_3 + b_{11}X_1^2 + b_{22}X_2^2 + b_{33}X_3^2 \quad \text{Eq. (1)}$$

The variable Y denotes the outcome that is measured for every combination of factor levels. The coefficient b_0 is the intercept parameter, and b_1, b_2, and b_3 denote the coefficients for linear regression. Denoted as b_{12}, b_{13}, and b_{23}, the coefficients correspond to the interaction regression coefficients, whereas b_{11}, b_{22}, and b_{33} indicate the coefficients for the quadratic

Table 1: Factors and responses used in BBD for the formulation of FNS

Variables	*Levels*		
Factors (Independent Variables)	-1	0	+1
X_1= Chitosan concentration (%w/v)	0.10	0.20	0.30
X_2= CS/TPP ratio	2:1	3:1	4:1
X_3 = Surfactant concentrations (%v/v)	1	2	3
Response (Dependent Variables):	*Constraints*		
Y_1 = Nanoparticle size (nm)	Minimize		
Y_2 = Particle size distribution (PDI)	Minimize		
Y_3 = %EE	Maximize		

Table 2: BBD layout for FNS formulation

Batch code	Formulation Variable			Responses		
	X_1	X_2	X_3	Y_1 (nm) mean ± SD	Y_2 mean ± SD	Y_3 (%) mean ± SD
FNS1[a]	0.2	3:1	2	125.3 ± 2.10	0.1430 ± 0.0532	94.73 ± 2.43
FNS2[a]	0.2	3:1	2	122.1 ± 1.52	0.1380 ± 0.0421	93.96 ± 3.71
FNS3	0.3	2:1	2	136.33 ± 1.56	0.4310 ± 0.3548	63.65 ± 6.34
FNS4	0.2	2:1	1	97.24 ± 1.87	0.2310 ± 0.3476	60.79 ± 4.76
FNS5[a]	0.2	3:1	2	121.42 ± 1.44	0.1390 ± 0.3467	93.88 ± 1.34
FNS6[a]	0.2	3:1	2	123.61 ± 1.56	0.1420 ± 0.4531	91.96 ± 2.56
FNS7	0.1	2:1	2	115.55 ± 2.34	0.2010 ± 0.0341	66.88 ± 2.56
FNS8	0.2	4:1	1	117.59 ± 3.15	0.2510 ± 0.4171	85.69 ± 3.98
FNS9	0.2	2:1	3	127.31 ± 2.33	0.4210 ± 0.0912	60.79 ± 7.43
FNS10	0.3	3:1	1	131.62 ± 4.29	0.6210 ± 0.0023	64.75 ± 6.55
FNS11	0.1	4:1	2	130.64 ± 2.34	0.2910 ± 0.1300	80.96 ± 3.54
FNS12	0.2	4:1	3	149.57 ± 5.67	0.4510 ± 0.0620	65.78 ± 4.61
FNS13	0.3	3:1	3	162.44 ± 4.62	0.6410 ± 0.1243	62.99 ± 5.42
FNS14[a]	0.2	3:1	2	122.37 ± 2.59	0.1370 ± 0.1118	94.71 ± 5.54
FNS15	0.1	3:1	1	103.48 ± 3.31	0.2910 ± 0.1823	77.55 ± 5.66
FNS16	0.3	4:1	2	157.77 ± 2.36	0.4010 ± 0.0064	85.88 ± 2.69
FNS17	0.1	3:1	3	149.69 ± 3.22	0.6310 ± 0.0082	60.89 ± 6.83

Where X_1, X_2, X_3, Y_1, Y_2, and Y_3 are mentioned in Table 1; [a] indicating the replicated centre points of design

regression. Based on the observed experimental values of Y, these coefficients are derived. The variables X_1, X_2, and X_3 are defined as independent variables. Expressions X_1X_2, X_1X_3, and X_2X_3 denote the interactions between variables X_1 and X_2, X_1 and X_3, and X_2 and X_3, correspondingly. In contrast, X_1^2, X_2^2, and X_3^2 denote quadratic terms. To graphically depict the influence of the independent variables on the dependent variables (measured responses), 3D response surface graphs were generated. The goal was to decrease the particle size and polydispersity index while maximizing the percentage of entrapment efficiency to optimize the formulation.[12]

Particle size and polydispersity index (PDI)

100µl aliquots from all nanosuspension batches were diluted with distilled water (900µl) and average particle size and polydispersity index were measured by Zeta sizer (Malvern Instruments, UK) at 25°C under a fixed scattering angle of 90°.[17-19] All experiments were performed thrice (n = 3).

Entrapment efficiency

The method described by Bhattamisra *et al*., (2020) was used to determine the amount of entrapped felbamate in all optimization batches. This method indirectly measured the entrapped Felbamate in FNS by quantifying the remaining free felbamate in the aqueous supernatant medium. To do this, 10 mL aliquots were subjected to ultracentrifugation at 20,000 rpm at 4°C for 60 min. The resulting clear supernatant was then diluted and analyzed using UV spectrophotometry at 257 nm wavelength to detect the free drug in the solution.[20,21]

The % EE (entrapment efficiency) was calculated using the equation provided below:

$$EE = \frac{Initial\ weight\ of\ drug\ (mg) - Free\ drug\ in\ supernatant\ (mg)}{Initial\ weight\ of\ drug\ (mg)} X100 \qquad \text{Eq. (2)}$$

In-vitro drug release study

The drug release study was conducted using a vertical Franz diffusion cell with a diffusion area of 1cm^2 and a capacity of 15 mL. For this study, a dialysis membrane (cutoff 2 KDa) was used. A total of 4 Franz diffusion assemblies were made for the study in which 3 Franz diffusion assemblies for the formulation (FNS) for triplicate results and one for control (pure drug aqueous suspension). A 1.55 cm^2 contact area dialysis membrane was affixed to the receptor compartment of each Franz diffusion cell. The receptor compartment of each Franz diffusion cell was filled with a phosphate buffer at a pH of 6.4. Each assembly was positioned on the magnetic stirrer and maintained at a temperature of 37 ± 0.5°C while being continuously stirred at 100 rpm. FNS equivalent to 5 mg of FBM was added to the donor compartment of each of the three Franz diffusion cells. The receptor compartment of the 4th Franz diffusion assembly was filled with a suspension of Pure FBM (5 mg) in phosphate buffer at a pH of 6.4. 1 ml of sample was withdrawn from the receptor compartment of each Franz diffusion cell at specified time intervals with the replacement of an equal volume of fresh phosphate buffer (pH 6.4) to maintain the sink condition. The samples were filtered

with Millipore and then analyzed by UV-Spectrophotometer at 257 nm wavelength for estimation of the amount of drug released as a function of time.[22]

RESULTS AND DISCUSSION

Formulation Preparation and Optimization of FNS

The BBD was utilized to establish the correlation between the concentration of CS (chitosan), the ratio of CS to sodium TPP (tripolyphosphate), and the concentration of surfactant on the response variables to optimize the felbamate nanosuspension for nose-to-brain targeting. The formulation variables and their observed responses are displayed in Table 2. The particle size (Y_1), polydispersity index (PDI) (Y_2), and percent encapsulation efficiency (%EE) (Y_3) for all the formulation batches varied between 97.24 ± 1.87 and 162.44 ± 4.62 nm; 0.137 and 0.641; and 60.79 ± 4.76 to 94.73 ± 2.43% respectively. The excellent consistency in FNS preparation and response analysis was demonstrated by the strong concordance among the five test replicates (FNS 1, 2, 5, 6, and 14).

Optimization of Formulation by BBD

Fitting response data to model statistics

The results of the 17 formulations were collectively fitted to linear, 2FI (two-factor interaction), quadratic, and cubic models. The R^2 value for the quadratic model was found to be greater than 0.9, and maximizing the adjusted R^2 and predicted R^2 values, revealed that the quadratic model provided the most accurate match to the data.

The ANOVA findings indicated that the quadratic model was significant and the lack of fit for the suggested quadratic model was not significant, as seen by the p-values for the model and lack of fit, respectively for each response. This suggests that the selected model fits well with the data. The ANOVA analysis revealed that the F ratio was greater and the p-value was smaller for the variables X_1, X_2, X_3, X_1X_3, and X_1^2, indicating their substantial impact on the response variables Y_1 (which represents nanoparticle size) and Y_2 (which represents polydispersity index). The effect of interaction factors X_1X_2, and X_2X_3; quadratic factors X_2^2 and X_3^2 were insignificant on particle size. The factors X_1X_2, X_2^2, and X_3^2 significantly affect the polydispersity index of nanoparticles. The interaction factor X_2X_3 was not significant for PDI. The factors X_2, X_3, X_1X_3, X_2X_3, X_1^2, X_2^2, and X_3^2 were significantly affect Y_3 (percentage entrapment efficiency of nanoparticles). The X_1X_2 and X_1 were insignificant for %EE. For each response, inputs for quadratic model parameters generated by the Design Expert software are given in Table 3.

Table 3: Projected values produced by design expert software

Quadratic model	R^2	*Adjusted* R^2	*Predicted* R^2	*SD*	*%CV*
Response (Y_1)	0.9904	0.9781	0.8735	2.62	2.03
Response (Y_2)	0.9997	0.9993	0.9961	0.0047	1.42
Response (Y_3)	0.9905	0.9783	0.8717	2.06	2.68

Analysis of response data

The coefficients and p-values of individual and combined factors provide a quantitative measure of the influence of each factor on the chosen responses (Table 4). The numerical value of the regression coefficient is the expected change in the response for every one unit change in the factor value while holding all other factors constant.

The quadratic model's polynomial regression equation (in terms of Actual factors) for individual responses was generated to quantify how much formulation variables affect individual responses (Equation 2-4).

$$\text{Particle size } (Y_1) = 80.7487 - 379.525\,X_1 + 11.065\,X_2 + 20.2425\,X_3 + 15.875\,X_1X_2 - 38.475\,X_1X_3 + 0.4775\,X_2X_3 + 1299.63\,X_1^2 - 0.88375\,X_2^2 + 0.85125X_3^2 \quad \text{(Eq. 2)}$$

$$\text{PDI } (Y_2) = 0.8075 - 4.624\,X_1 + 0.11765\,X_2 - 0.58115\,X_3 - 0.3 * X_1X_2 - 0.8\,X_1X_3 + 0.0025\,X_2X_3 + 19.935\,X_1^2 - 0.00815\,X_2^2 + 0.20685\,X_3^2 \quad \text{(Eq. 3)}$$

$$\text{EE\% } (Y_3) = -111.14 + 277.573\,X_1 + 67.519\,X_2 + 69.4572\,X_3 + 20.375\,X_1X_2 + 37.25\,X_1X_3 - 4.9775\,X_2X_3 - 4.9775\,X_1^2 - 8.894\,X_2^2 - 16.6915\,X_3^2 \quad \text{(Eq. 4)}$$

Effect of formulation variables on response Y_1 (Particle Size)

Nanoparticle size analysis revealed a range of 97.24 to 162.44 nm (Table 2), satisfying the desired range (10–300 nm) for nose-to-brain delivery of felbamate [(4)]. It was observed that the nanoparticle size was dependent upon the concentration of CS, CS/TPP ratio, and surfactant concentration, where the lowest nanoparticle size (97.24 nm) corresponds to the 0.2% CS concentration, lowest CS/TPP ratio (2:1) and lowest surfactant concentration (1%). The positive and negative signs preceding each term in the regression equation indicate the positive and negative impact on the response variable.

The regression equation developed by Design Expert (Equation 2) showed that nanoparticle size (Y_1) was inversely related to CS concentration (X_1) and directly related to CS/TPP ratio (X_2) and surfactant concentration (X_3). This equation's intercept was 80.7487. The intercept was nanoparticle size when all independent variables (X_1, X_2, and X_3) were zero. The coefficient of Chitosan Concentration (X_1) was -379.525, indicating aggregation at higher concentrations. X_2 coefficient of 11.065 indicated that the CS/TPP ratio increased particle size. The 20.2425 coefficient of X_3 indicated that increased Tween 80 concentrations caused bigger particle sizes. Tween 80 concentrations from 0.1 to 0.3% v/v cause particle agglomeration. This may be due to FNS surfactant saturation. The particles aggregate because they are mostly adsorbed on the surfactant. The coefficient of X_1X_2 was 15.875. A positive number meant X_1 and X_2 increased particle size. The X_1X_3 coefficient was -38.475. A negative score indicated X_1 and X_3 reduced particle size. The X_2X_3 coefficient was 0.4775. A positive result meant X_2 and X_3 increased particle size.

Table 4: Regression coefficient values for FNS

Independent variables	*Size of nanoparticles (nm)*		*Particle size distribution (PDI)*		*Entrapment Efficiency (EE %)*	
	Regression coefficient	*p-value*	*Regression coefficient*	*p-value*	*Regression coefficient*	*p-value*
Intercept	122.96	< 0.0001	0.1398	< 0.0001	93.848	< 0.0001
X_1	11.1	< 0.0001	0.0850	< 0.0001	-1.12625	0.1660
X_2	9.8925	< 0.0001	0.0138	< 0.0001	8.275	< 0.0001
X_3	17.385	< 0.0001	0.0938	< 0.0001	-4.79125	0.0003
X_1X_2	1.5875	0.2655	-0.0300	< 0.0001	2.0375	0.0885
X_1X_3	-3.8475	0.0219	-0.0800	< 0.0001	3.725	0.0086
X_2X_3	0.4775	0.7266	0.0025	0.3186	-4.9775	0.0019
X_1^2	12.9962	< 0.0001	0.1994	< 0.0001	-10.6115	< 0.0001
X_2^2	-0.88375	0.5117	-0.0082	0.0088	-8.894	< 0.0001
X_3^2	0.85125	0.5269	0.2069	< 0.0001	-16.6915	< 0.0001

The quadratic factors X_1^2 and X_3^2 had positive coefficients of 1299.63 and 0.85125, respectively, demonstrating that raising each variable's squared value increased particle sizes. X_2^2's positive coefficients (-0.88375) show that increasing each variable's squared value reduces particle sizes.

Response surface methodology employed 3D model graphs to depict the influence of formulation variables on responses. By fixing one variable, the plots allowed for a qualitative assessment of how the remaining two variables interact and impact the dependent response. The 3D response surface plot (Figure 1A-C) shows how independent variables affect particle size. Two independent variables (X_1 and X_2) and a dependent response variable (particle size) are shown in Figure 1A. The surface color gradient showed particle size response values at different X_1 and X_2 combinations. Blue areas had smaller particles, whereas red spots had larger ones. The plot showed that chitosan concentration (X_1) increases particle size (red spots). As expected, increased chitosan concentrations cause agglomeration and bigger particles. The surface plot also demonstrated that a higher CS/TPP ratio (X_2) increases particle sizes (red spots). Chitosan excess may cross-link TPP molecules, resulting in bigger particles. The relationship between X_1 and X_2 was critical. Due to combination actions, increased chitosan concentration and CS/TPP ratio may increase particle size.

Figure 1B shows the link between the independent variables (X_1 and X_3) and the dependent variable (particle size). Increased chitosan concentration (X_1) leads to bigger particle sizes (red spots). This supports the idea that increased chitosan concentrations cause particle aggregation and size. Higher Tween 80 (X_3) concentrations increase particle sizes (red regions). Tween 80, a surfactant, aggregates particles at high concentrations. The interplay between X_1 and X_3 matters. High chitosan and Tween 80 concentrations may increase particle size due to combination effects. Figure 1C shows the association between CS/TPP ratio, Tween 80 conc. (%v/v), and particle size. The plot showed that raising the CS/TPP ratio increases particle sizes (red regions). Again, increased Tween 80 concentrations result in bigger particles (red spots). Also important is X_2 and X_3 interaction. If the CS/TPP ratio and Tween 80 concentration are high, combined impacts may increase particle size.

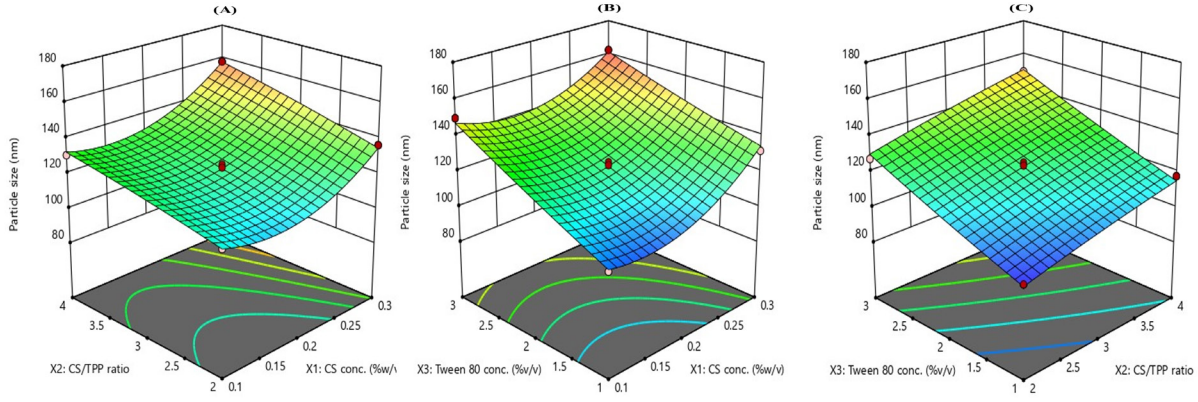

Figure 1: The impact of formulation variables (X_1, X_2 and X_3) on Particle Size (Responses Y_1)

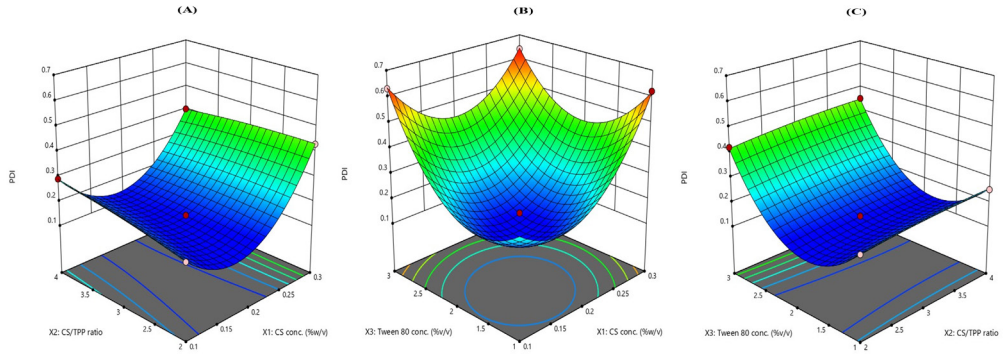

Figure 2: The impact of formulation variables (X_1, X_2 and X_3) on Polydispersity Index (Responses Y_2)

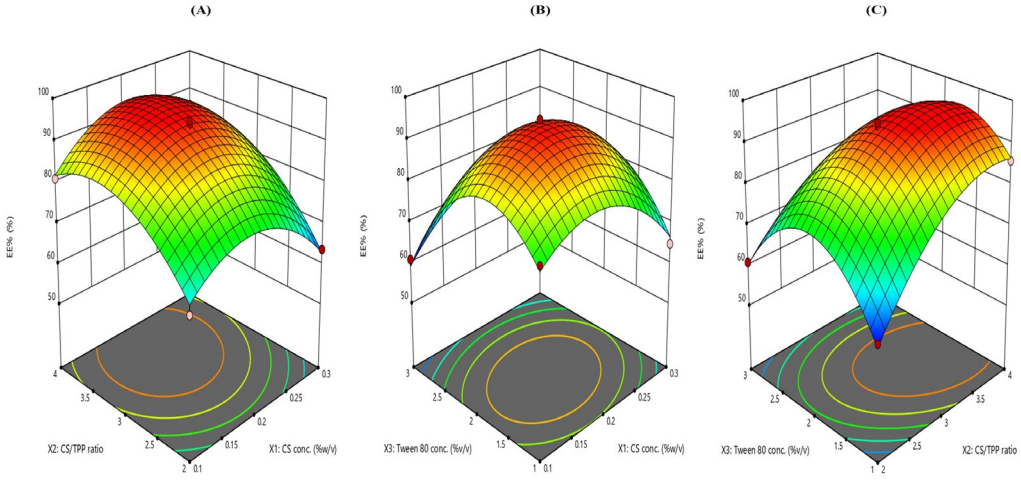

Figure 3: The impact of formulation variables (X_1, X_2 and X_3) on %Entrapment Efficiency (Responses Y_3)

Effect of formulation variables on response Y_2 (PDI)

All 17 formulations had PDIs between 0.137 and 0.641 (Table 2). The regression equation developed by Design Expert showed that polymer concentration (X_1) inversely affected PDI (Y_2), whereas CS/TPP ratio (X_2) and surfactant concentration (X_3) did not. The baseline PDI value when all predictor variables (X_1, X_2, X_3) were zero was 0.8075 in this regression equation. X_1's negative coefficient (-4.624) showed that PDI decreases with chitosan content. A positive coefficient (0.11765) of X_2 showed that raising the CS/TPP ratio somewhat raises PDI. Higher Tween 80 concentration decreased PDI, according to X_3's negative coefficient (-0.58115). The interaction term X_1X_2 (-0.3) revealed that CS/TPP ratio affected chitosan concentration. Tween 80's influence on chitosan concentration was reflected by the interaction term X_1X_3 (-0.8). Quadratic terms (X_1^2, X_2^2, X_3^2) caused non-linear effects. Their coefficients represented response surface curvature.

The 3D response surface plot (Figure 2A-C) shows how independent variables affect particle size. Figure 2A shows the association between two independent variables (X_1 and X_2) and Y_2 (PDI). PDI decreased as CS concentration increased, according to the plot. Lower nanoparticle PDI values suggested a narrower size distribution. High-CS concentrations produced more uniform particles. Encapsulation and particle size were improved by CS. Minimizing PDI required an ideal CS/TPP ratio. Deviating from this optimal ratio may broaden size distributions. Because the optimum mix ensures nanoparticle stability and cross-linking. Too much or too little TPP may influence particle size. The surface curvature showed CS conc. and CS/TPP ratio interactions. The lowest PDI was at certain CS concentrations and CS/TPP ratios.

The link between X_1 and X_3, two independent variables, and Y_2 (PDI), a dependent response variable, is shown in Figure 2B. Increased CS concentration lowered PDI. High-CS concentrations produced more uniform particles. Encapsulation and particle size were improved by CS. Initial PDI reduction may increase with Tween 80 content. However, after reaching an appropriate concentration, increasing it further could result in higher PDI. Nanoparticles become more stable and dispersible with Tween 80. Insufficient Tween 80 may impair dispersion and affect PDI. Too much Tween 80 can disturb encapsulation or create instability. The surface curvature showed CS and Tween 80 interactions. Specific CS and Tween 80 concentrations yielded the lowest PDI.

In Figure 2C, PDI (Y_2) is a dependent response variable to two independent variables, X_2: CS/TPP ratio and X_3: Tween 80 conc. (%v/v). The plot showed that PDI increased with Tween 80 concentration. Blue (lower PDI) to green (greater PDI)

along the x-axis showed this. PDI increased with the CS/TPP ratio. The y-axis color change from blue to green reflects this. The curved surface showed that Tween 80 concentration and CS/TPP ratio affected PDI. We observed blue areas where PDI was lowest at certain concentrations and ratios. Beyond those marks, PDI increased (green).

Effect of Formulation Variables on Response Y_3 (EE%)

All 17 formulations had EE%s between 60.79 and 94.73% (Table 2). The regression equation (Eq. 4) developed by the Design Expert showed that polymer concentration (X_1), CS/TPP ratio (X_2), and surfactant concentration (X_3) directly affected EE% (Y_3). Entrapment Efficiency (EE%) was baselined at -111.14% when all predictor variables (X_1, X_2, X_3) were zero. A positive X_1 coefficient (277.573) suggested that EE% increased with X_1. A positive X_2 coefficient (67.519) indicated a small increase in EE%. Positive X_3 coefficients (69.4572) indicated higher EE%. The interaction term X_1X_2 (20.375) suggested that X_1's effect depends on X_2. The interaction term X_1X_3 (37.25) showed that X_1 and X_3 affected EE%. The interaction term X_2X_3 (-4.9775) showed that X_3's influence depends on X_2. The quadratic term (X_1^2, X_2^2, X_3^2) contributed non-linearly to EE%.

The Figure 3(A-C) 3D response surface plot shows how independent variables affect EE%. Y_3 (EE%) is dependent on two independent factors (X_1 and X_2), as shown in Figure 3A. Increasing X_1 may raise EE% to a point. After that, increasing X_1 may not improve EE% or perhaps reduce it. At low concentrations, CS may not be enough to encapsulate the active ingredient. FBM encapsulation rises with CS concentration. At high concentrations, aggregation or other problems may impair EE%. The best CS/TPP ratio varies on the system and formulation. A good CS/TPP ratio was important since too low a ratio could produce incomplete cross-linking and inadequate encapsulation, while too high could induce excessive cross-linking and lower EE%.

A dependent response variable Y_3 (%EE) is related to two independent variables (X_1 and X_3) in Figure 3B. As CS concentration (X_1) increased, EE% improved partially. After that optimal concentration, EE% may not improve or may even drop. It may have been because low CS concentrations were inadequate to encapsulate the active ingredient. More drug can be enclosed with higher CS concentrations. However, large CS concentration may create aggregation or other problems, lowering EE%. Tween 80 concentration may initially boost EE%. Beyond an appropriate concentration, increasing may lower EE%. Nanoparticles become more stable and dispersible with Tween 80. Poor dispersion from too little Tween 80 can affect EE%. Too much Tween 80 can disturb encapsulation or create instability. The surface curvature showed CS and Tween 80 interactions. Specific CS and Tween 80 concentrations yielded the maximum EE%.

Figure 3C shows the relationship between Y_3, a dependent response variable, and two independent components, X_2: CS/TPP ratio and X_3: Tween 80 conc. (%v/v). The plot showed that low CS/TPP ratios may cause incomplete cross-linking and poor encapsulation. High ratios can produce excessive cross-linking, reducing EE%. Initial Tween 80 concentration may enhance EE%. Increases may lower EE% beyond a certain concentration. Insufficient Tween 80 dispersion affects EE%. Too much Tween 80 can disrupt encapsulation or cause instability. Surface curvature indicated CS/TPP-Tween 80 concentration correlations. The highest EE% was found at particular CS/TPP ratios and Tween 80 concentrations.

Validation of the optimization model

Specific parameters were entered into Design Expert to generate the expected composition. The goals were the highest encapsulation efficiency (%EE), the most favorable particle size, and the lowest polydispersity index. Based on desirability values, software-recommended values were selected as a zone of interest and verified.

The optimized formulation was calculated by numerical method through Design Expert. Following optimization of X_1, X_2, and X_3 (as demonstrated in Table 5), the software's estimated desirability value was found to be 0.904, suggesting a 90.40% chance of accomplishing the goal.

The tween 80 concentration was established at 1.55% (v/v), and the design space was generated by adjusting the other two parameters. The Design Expert software generates an overlay plot (Figure 4) that illustrates the design space for choosing the best concentration of variables to formulate a Felbamate nanosuspension with enhanced stability, smaller particle size, and improved entrapment efficiency. In Figure 4, the bright yellow color defines the acceptable factor setting where response criteria can be met. Grey color defines the unacceptable factor settings. The dark yellow color in the overlay plot represents the area where different optimal regions overlap. It corresponds to the sweet spot, where the optimal factor level is present for optimal nanosuspension formulation.

The final formulation was prepared with optimized CS concentration, CS/TPP ratio, and Tween 80 concentration, and its responses were analyzed. The average particle size of the produced optimized FNS was 115.0 ± 4.37 nm. Particle size distribution was also uniform, as seen by the PDI value (0.118 ± 0.021) being less than 0.5. The entrapment efficiency of the optimized formula was found to be 90.32 ± 4.69 %, which was near to the predicted values proposed by Design Expert software.

The summary of optimization is given in Table 6 where Actual levels are the optimized parameter and the coded levels are given by software. The design also suggested predicted

Table 5: Optimized formula given by design expert software using box-behnken design

S.No.	*CS conc.*	*CS/TPP ratio*	*Tween 80 conc.*	*Particle size*	*PDI*	*EE%*	*Desirability*	*Desirability (w/o Intervals)*
1	0.176	3.338	1.553	116.039	0.127	95.067	0.904	0.925

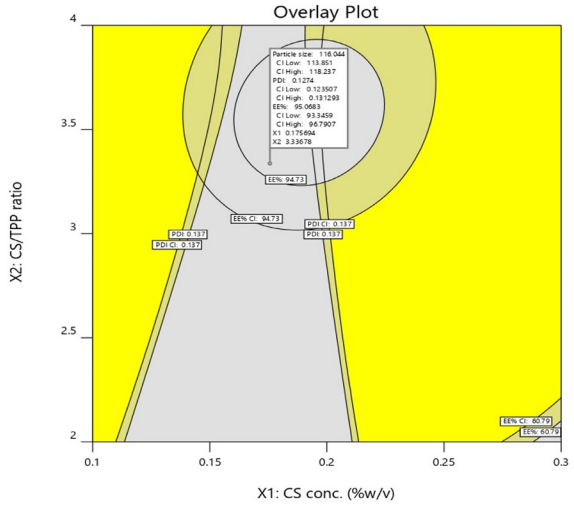

Figure 4: The overlay plot provided by design expert software displays the design space shaded in yellow

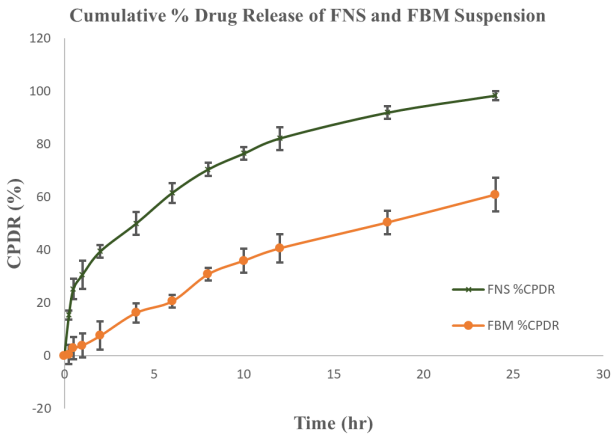

Figure 5: Cumulative percentage drug release from FBM suspension and FNS

Table 6: Responses at optimum conditions: experimental and predicted values

Optimum conditions	*Coded levels*	*Actual levels*
Chitosan concentration (%w/v)	- 1.824	0.176
CS/TPP ratio	0.3	3.3:1
Surfactant concentrations (%v/v)	- 0.45	1.55
Response	Predicted values	Experimental values
Nanoparticle size (nm)	116.048	115.0 ± 4.37 nm
Polydispersity Index (PDI)	0.127	0.118 ± 0.021
%EE	95.069	90.32 ± 4.69 %

response values of these optimized parameters which was confirmed by formulating the FNS using optimized parameters. The coded levels were calculated by using the equation 5.

$$Z = Z_0 - \frac{Z_C}{\Delta Z} \qquad \text{(Eq. 5)}$$

The coefficients Z and Z_0 denote the encoded and real levels of the independent variables, respectively. A step shift is denoted by ΔZ, while the actual values at the central point are shown by Z_c.

In-vitro drug release study

Using a release medium (phosphate buffer 6.4), chitosan nanoparticles were incubated and their Felbamate release behavior was evaluated using UV spectrophotometry. The release profiles of felbamate are shown in Figure 5 for incubation times of up to 24 hours. After 0.5 hours, only 2.8 ± 4.23% of the drug had been released in the case of pure Fb suspension. In Figure 5, we can see that the initial burst release of Felbamate from FNS was 25.246 ± 3.77% after 0.5 hours in all incubation media. Felbamate was initially rapidly released, defined as a "burst effect," because some amounts were concentrated on the surface of nanoparticles via adsorption and were then easily released via diffusion. The total amount released over the incubation period was 98.3745 ± 0.66% after an initial burst effect that was followed by a slower sustained and controlled release.

CONCLUSION

The experimental approach facilitated the systematic optimization of the nanosuspension formulation by identifying the physicochemical characteristics that are crucial for achieving a stable felbamate nanosuspension with both high efficacy and the capacity to target the brain through the nose. The design assessed the key variables affecting observed responses and examined the correlation between each of these variables using response surface methods. The Statistical optimization of formulation parameters and assessment of the major interaction and quadratic effects of independent variables on particle size, polydispersity index, and entrapment efficiency of felbamate nanosuspension were successfully achieved using the Box-Behnken design. This study utilized a 3-factor, 3-level design to examine the response surfaces of linear and quadratic functions and to construct a second-order polynomial model. Based on the results of the experiments and the desirability criteria, the optimum formulation of felbamate nanosuspension for nose-to-brain delivery of drugs was found to be 0.176% chitosan solution, 3.3:1 chitosan/TPP ratio, and 1.55% Tween 80. The in-vitro dissolution investigations of the optimized nanosuspension demonstrated a significantly higher dissolution rate compared to the pure felbamate suspension, indicating a potential improvement in the bioavailability of felbamate.

ACKNOWLEDGMENT

We express our gratitude to the Institute of Pharmacy of Bundelkhand University where this work was conducted and thankful to my supervisor Dr. Rishikesh Gupta, Assistant Professor, Assistant Professor, Institute of Pharmacy, Bundelkhand University and all those who have supported and guided me in the journey of my research work.

REFERENCES

1. Reed L, Ciliberto M, Fong SL, Nickels K, Kossoff E, Wirrell E, *et al*. Efficacy of felbamate in a cohort of patients with epilepsy with myoclonic atonic seizures (EMAtS). Epilepsy Res. 2024 Mar 1;201:107314. https://doi.org/10.1016/j.eplepsyres.2024.107314
2. Löscher W, Sills GJ, White HS. The ups and downs of alkyl-carbamates in epilepsy therapy: How does cenobamate differ? Epilepsia. 2021 Mar 13;62(3):596–614. https://doi.org/10.1111/epi.16832
3. Leppik IE, White JR. Felbamate. In: The Treatment of Epilepsy. Wiley; 2015. p. 472–8. https://doi.org/10.1002/9781118936979.ch35
4. Boyuklieva R, Pilicheva B. Micro- and Nanosized Carriers for Nose-to-Brain Drug Delivery in Neurodegenerative Disorders. Biomedicines. 2022 Jul 14;10(7):1706. https://doi.org/10.3390/biomedicines10071706
5. Maurya P, Mittal A, Sharma K, Alam S. Fabrication of Acetazolamide Loaded Nasal Nanosuspension : an *in-vitro* and Ex Vivo Characterization. Analele Univ "Dunărea Jos" Galați. 2013;17(1):93–105.
6. Pandey A, Nikam A, Basavraj S, Mutalik S, Gopalan D, Kulkarni S, *et al*. Nose-to-brain drug delivery: Regulatory aspects, clinical trials, patents, and future perspectives. In: Direct Nose-to-Brain Drug Delivery: Mechanism, Technological Advances, Applications, and Regulatory Updates. Elsevier; 2021. p. 495–522. https://doi.org/10.1016/B978-0-12-822522-6.00023-0
7. Shringarpure M, Gharat S, Momin M, Omri A. Management of epileptic disorders using nanotechnology-based strategies for nose-to-brain drug delivery. Vol. 18, Expert Opinion on Drug Delivery. Taylor & Francis; 2021. p. 169–85. https://doi.org/10.1080/17425247.2021.1823965
8. Maurya P, Gupta R, Mahor A. Felbamate Chitosan Nasal Nanosuspension: an in-Vitro and in-Vivo Evaluation. African J Biol Sci (South Africa). 2024;6(April):399–412. doi: 10.33472/AFJBS.6.1.2024.399-412
9. Chelladurai SJS, Murugan K, Ray AP, Upadhyaya M, Narasimharaj V, Gnanasekaran S. Optimization of process parameters using response surface methodology: A review. In: Materials Today: Proceedings. Elsevier; 2020. p. 1301–4. https://doi.org/10.1016/j.matpr.2020.06.466
10. Pongsumpun P, Iwamoto S, Siripatrawan U. Response surface methodology for optimization of cinnamon essential oil nanoemulsion with improved stability and antifungal activity. Ultrason Sonochem. 2020 Jan;60(April 2019):104604. https://doi.org/10.1016/j.ultsonch.2019.05.021
11. Ashar F, Hani U, Osmani RAM, Kazim SM, Selvamuthukumar S. Preparation and Optimization of Ibrutinib-Loaded Nanoliposomes Using Response Surface Methodology. Polymers (Basel). 2022 Sep 17;14(18):3886. https://doi.org/10.3390/polym14183886
12. Venkatasubramaniyan C, Kumar SS. Design and Development of Chitosan Based Etravirine Nanosuspension. Nanomedicine Res J. 2022;7(3):270–87. DOI: 10.22034/nmrj.2022.03.007
13. Raghavendra Naveen N, Kurakula M, Gowthami B. Process optimization by response surface methodology for preparation and evaluation of methotrexate loaded chitosan nanoparticles. In: Materials Today: Proceedings. Elsevier; 2020. p. 2716–24. https://doi.org/10.1016/j.matpr.2020.01.491
14. Algharib SA, Dawood A, Zhou K, Chen D, Li C, Meng K, *et al*. Preparation of chitosan nanoparticles by ionotropic gelation technique: Effects of formulation parameters and *in-vitro* characterization. J Mol Struct. 2022 Mar 15;1252:132129. https://doi.org/10.1016/j.molstruc.2021.132129
15. Barnabas W. Drug targeting strategies into the brain for treating neurological diseases. J Neurosci Methods. 2019 Jan 1;311:133–46. https://doi.org/10.1016/j.jneumeth.2018.10.015
16. Masjedi M, Azadi A, Heidari R, Mohammadi-Samani S. Brain targeted delivery of sumatriptan succinate loaded chitosan nanoparticles: Preparation, *In-vitro* characterization, and (Neuro-)pharmacokinetic evaluations. J Drug Deliv Sci Technol. 2021 Feb 1;61:102179. https://doi.org/10.1016/j.jddst.2020.102179
17. Powar TA, Hajare AA. QbD Based Approach to Enhance the In-Vivo Bioavailability of Ethinyl Estradiol in Sprague-Dawley Rats. Acta Chim Slov. 2020 Mar 20;67(1):283–303. DOI: 10.17344/acsi.2019.5441
18. Ding Z, Mo M, Zhang K, Bi Y, Kong F. Preparation, characterization and biological activity of proanthocyanidin-chitosan nanoparticles. Int J Biol Macromol. 2021 Oct 1;188:43–51. https://doi.org/10.1016/j.ijbiomac.2021.08.010
19. Guo H, Li F, Qiu H, Liu J, Qin S, Hou Y, *et al*. Preparation and Characterization of Chitosan Nanoparticles for Chemotherapy of Melanoma Through Enhancing Tumor Penetration. Front Pharmacol. 2020 Mar 13;11(March):1–8. . doi: 10.3389/fphar.2020.00317
20. Othman N, Masarudin MJ, Kuen CY, Dasuan NA, Abdullah LC, Md. Jamil SNA. Synthesis and Optimization of Chitosan Nanoparticles Loaded with l-Ascorbic Acid and Thymoquinone. Nanomaterials. 2018 Nov 7;8(11):920. https://doi.org/10.3390/nano8110920
21. Bhattamisra SK, Shak AT, Xi LW, Safian NH, Choudhury H, Lim WM, *et al*. Nose to brain delivery of rotigotine loaded chitosan nanoparticles in human SH-SY5Y neuroblastoma cells and animal model of Parkinson's disease. Int J Pharm. 2020 Apr 15;579:119148. https://doi.org/10.1016/j.ijpharm.2020.119148
22. Saha P, Singh P, Kathuria H, Chitkara D, Pandey MM. Self-Assembled Lecithin-Chitosan Nanoparticles Improved Rotigotine Nose-to-Brain Delivery and Brain Targeting Efficiency. Pharmaceutics. 2023 Mar 5;15(3):851. https://doi.org/10.3390/pharmaceutics15030851